

LOSS OF LINEAR MOMENTUM IN AN ELECTRODYNAMICS SYSTEM: FROM AN ANALYTICAL APPROACH TO SIMULATIONS

D. S. H. Charrier

Department of Physics and Mechanics of Materials
University of Poitiers
Bat. SP2MI, Bd Marie et Pierre Curie, BP 30179
Futuroscope 86962, France

Abstract—The classical electrodynamics allows the use of retarded electromagnetic fields. The purpose of this investigation is to predict the useful force in a coil-ring system by electromagnetomechanical conversion. Analytical equations in retarded regime are given and are used to simulate a realistic thruster based on the coil-ring system. It is shown that a net force in the inertial coil-ring system is created. By means of high frequency electronics, analytical and practical tools toward new experiments for electromagnetic thrusters are given.

1. INTRODUCTION

In this paper, a question arises: is it possible to create a thrust [1] using retarded electromagnetic fields in an inertial system without exerting an external force? An ultra fast current ramp in an emitter coil induces a repulsive force in a receptor coaxial conductive disc or ring. Using this principle, magnetic actuators can provide high forces reported until 130 000 N [2]. This force is not anecdotal and motivates this work. The aim is to convert a part or the whole force into a real thrust using the property of retarded fields. A gedankenexperiment is proposed and simulated. Due to the retarded field there is a loss of the momentum not only on short time scales (ns) but on long times ($>$ seconds). The causality of a physical phenomenon is still source of fascinating debates and has theoretical consequences that are controversial in modern gravitation theories [3]. Here, the coil-ring

Corresponding author: D. S. H. Charrier (dscharrier@free.fr).

problem is treated from the retarded waves travel until resultant force calculations.

Into the frame of classical electrodynamics, the explanation of the created force in the coil-ring system may be detailed considering the retarded regime. Thus, the current pulse generates a spectrum of electromagnetic waves that leave the coil, covers the coil-to-ring distance at light speed and reaches the conductive ring surface. Here, it induces eddy currents which become the source of repulsive electromotive force. The newly created electromagnetic spectrum covers back the ring-to-coil distance at light speed to produce an induced current in the coil and so on. The electromagnetic waves in retarded regime for time dependent current distributions are entirely described by the generalized Jefimenko equations [4] (also called Heaviside-Feynman formula [5]). These equations take into account retardation effects becoming important at extremely high frequencies, by essence. At lower frequencies the retardation can be neglected. It is shown in the paper that only high frequencies (> 3 GHz) are involved, by looking at the spatial scales. The retarded fields were mainly studied in particle physics [6–9] and for moving atomic dipoles [10, 11]. More recently, Jiménez et al. [12] gave the exact electromagnetic field in retarded and static regime produced by a finite wire. So far, the electromagnetic field produced by a single circular ring in retarded coordinates with a time dependent current has not been reported in the literature. In this study, the dimension of wire sections is very small compared to the diameter of rings.

In the second part, the generalized equations of Jefimenko are given for one emitter ring in transient regime. In the third part, the induced electromotive force acting on a receptor ring and the generalized equations of Jefimenko for the single ring situation are simulated. The simulations show that the net force between an emitter ring and a receptor ring is not equal to zero. In the last part, the case of a realistic thruster is discussed using a magnetic core.

2. EXPRESSIONS OF THE RETARTED FIELD OF A SINGLE RING

The Jefimenko equations give the exact expressions of retarded electric $\vec{E}(\vec{x}, t)$ and magnetic $\vec{B}(\vec{x}, t)$ fields in space and time created by a transient (time dependent) current distribution. They are generally

written as follows [13, 14]:

$$\vec{E}(\vec{x}, t) = \frac{1}{4\pi\epsilon_0} \int d^3x' \left\{ \frac{\vec{R}}{R^3} [\alpha(\vec{x}', t')]_{ret} + \frac{\vec{R}}{cR^2} \left[\frac{\partial\alpha(\vec{x}', t')}{\partial t'} \right]_{ret} - \frac{1}{c^2R^2} \left[\frac{\partial\vec{J}(\vec{x}', t')}{\partial t'} \right]_{ret} \right\} \quad (1)$$

$$\vec{B}(\vec{x}, t) = \frac{\mu_0}{4\pi} \int d^3x' \left\{ [\vec{J}(\vec{x}', t')]_{ret} \wedge \frac{\vec{R}}{R^3} + \left[\frac{\partial\vec{J}(\vec{x}', t')}{\partial t'} \right]_{ret} \wedge \frac{\vec{R}}{cR^2} \right\} \quad (2)$$

where ϵ_0 and μ_0 are respectively the electric and magnetic constants, c is the light velocity, α the charge density and \vec{J} the current density. R ($|\vec{R}| = |\vec{x} - \vec{x}'|$) is the distance separating the current sources and observation points while $(\vec{x}', t' = t - |\vec{x} - \vec{x}'|/c)$ denotes the (retarded) coordinates of the current source where the electromagnetic waves traveling at light speed are created.

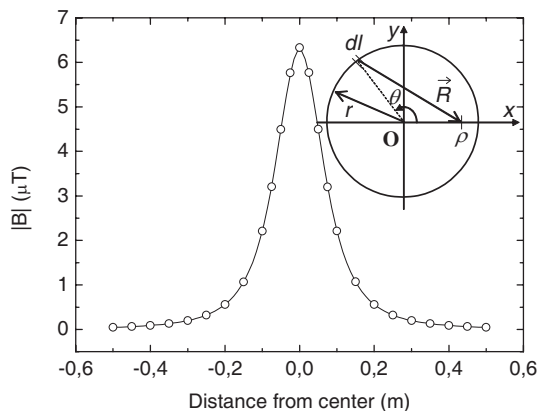


Figure 1. Continuous line: norm of magnetic field along z axis according to the known Biot-Savart equation for a ring radius $r = 10$ cm and a current $i = 1$ A. Empty circles: norm of magnetic field using Eq. (6) with the same parameters and with $B_z = \lim_{\rho \rightarrow 0} B_z(\rho, z, t)$.

The inset shows the ring in the (Oxy) plane, the cylindrical coordinates (z, θ, ρ) , the ring radius r and the observation point \vec{R} .

The particular case of a ring with a transient current i is analyzed using the cylindrical coordinates (z, θ, ρ) (see also the inset of Fig. 1):

$$\begin{cases} \vec{R} = (|\rho| - r \cos \theta) \vec{u}_x - r \sin \theta \vec{u}_y + z \vec{u}_z \\ \vec{J}(\vec{x}', t') d^3x' = J(\vec{x}', t') dS d\vec{l} = i(\vec{x}', t') dl' \vec{u}_\theta \end{cases} \quad (3)$$

where r is the ring radius, S the ring section and dl the unit length of the ring. Now, let's define the vector \vec{R} : since the problem is cylindrical, the integration can be done on one plan passing through the z plan. The drawing in inset of Fig. 1 suggests the x axis is taken as integration axis. Then the vector \vec{R} points from the integration element dl to the plan Oxz located at (ρ, z) . As there is no charge density in the ring ($\alpha = 0$) and injecting Eq. (3) into Eqs. (1) and (2), the analytical electromagnetic field in transient regime created by a ring is written in cylindrical coordinates:

$$E_\theta(\rho, z, t) = -\frac{1}{4\pi\epsilon_0 c^2} \frac{1}{2|\rho|} \int \left[\frac{\partial i(\vec{x}', t')}{\partial t'} \right]_{ret} \frac{d\theta}{(a - \cos \theta)} \quad (4)$$

$$\begin{aligned} B_\rho(\rho, z, t) = \frac{\mu_0 r z}{4\pi} & \left(\frac{1}{(2r|\rho|)^{3/2}} \int_{-\pi}^{\pi} [i(x', t')]_{ret} \frac{\cos \theta d\theta'}{(a - \cos \theta)^{3/2}} \right. \\ & \left. + \frac{1}{2cr|\rho|} \int_{-\pi}^{\pi} \left[\frac{\partial i(x', t')}{\partial t'} \right]_{ret} \frac{\cos \theta d\theta'}{a - \cos \theta} \right) \end{aligned} \quad (5)$$

$$\begin{aligned} B_z(\rho, z, t) = \frac{\mu_0 r}{4\pi} & \left(\frac{1}{(2r|\rho|)^{3/2}} \left(\int_{-\pi}^{\pi} [i(x', t')]_{ret} \frac{rd\theta'}{(a - \cos \theta)^{3/2}} - \int_{-\pi}^{\pi} [i(x', t')]_{ret} \frac{|\rho| \cos \theta d\theta'}{(a - \cos \theta)^{3/2}} \right) \right. \\ & \left. + \frac{1}{2cr|\rho|} \left(\int_{-\pi}^{\pi} \left[\frac{\partial i(x', t')}{\partial t'} \right]_{ret} \frac{rd\theta'}{a - \cos \theta} - \int_{-\pi}^{\pi} \left[\frac{\partial i(x', t')}{\partial t'} \right]_{ret} \frac{|\rho| \cos \theta d\theta'}{a - \cos \theta} \right) \right) \end{aligned} \quad (6)$$

with $a \equiv \frac{\rho^2 + z^2 + r^2}{2|\rho|r}$.

Equations (4)–(6) are the generalized equations of Jefimenko for a single ring with transient current. To confirm the consistence of Eqs. (4)–(6), the analytical Biot-Savart expression of the magnetic field along the z axis of the ring with a DC current $B_z(\rho = 0) = \mu_0 i r^2 / [2(r^2 + z^2)^{3/2}]$ should be recovered from Eq. (6) by fixing the boundary condition $\partial i / \partial t = 0$ and $\rho \rightarrow 0$. The numerical calculations of elliptical functions were done with Mathematica 6. In Fig. 1, the continuous curve is the magnetic field according to the analytical

equation. The empty circles are the numerical calculated points using Eq. (6) with $B_z = \lim_{\rho \rightarrow 0} B_z(\rho, z, t)$. The good agreement between the known analytical expression and the calculated one is a first validation of Eq. (6). As an additional check, far from the coil the expression of the fields should approach those of a radiating magnetic dipole. For that let's define the magnetic dipole moment of the ring $\vec{m} = \pi r^2 i \vec{u}_z$. The static magnetic dipole assumes a constant current $\partial i / \partial t = 0$ and a negligible ring radius $|\vec{R}| \gg r$. With the later conditions, Eqs. (5) and (6) should be identical with those reported in literature $B_x = \mu_0 3m x z / (4\pi(x^2 + z^2)^{5/2})$ and $B_z = \mu_0 m(2z^2 - x^2) / (4\pi(x^2 + z^2)^{5/2})$ [15]. Because of cylindrical symmetry, the radial components are equal ($B_x = B_y$). The magnetic field of a dipole moment is shown in Fig. 2. Four dashed lines are indexed with letters A, B, C and D. The rescaled magnetic field $\sqrt{B_x^2 + B_z^2} / \mu_0 m$ of magnetic field through these dashed lines are shown in Figs. 3 (a) and (b) in arbitrary units. Using Mathematica, the Figs. 3 (a) and (b) show the analytical curves (lines) versus the numerical points (symbols). The numerical points are obtained with Eqs. (5) and (6) using the dipole approximations $|\vec{R}| \gg r$ and $\partial i / \partial t = 0$. The good agreement between analytical and numerical calculations is a second validation of Eqs. (5) and (6). Further on, a force study gives the estimation of net thrust between two coaxial rings.

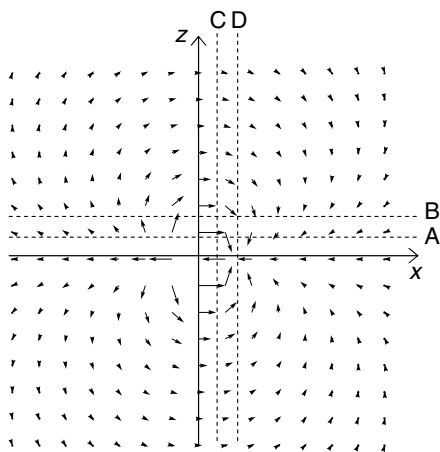


Figure 2. Magnetic dipole moment centered at $(x; z) = (0; 0)$ using Eqs. (5) and (6). The four dashed lines are indexed A, B, C and D. See text for more info.

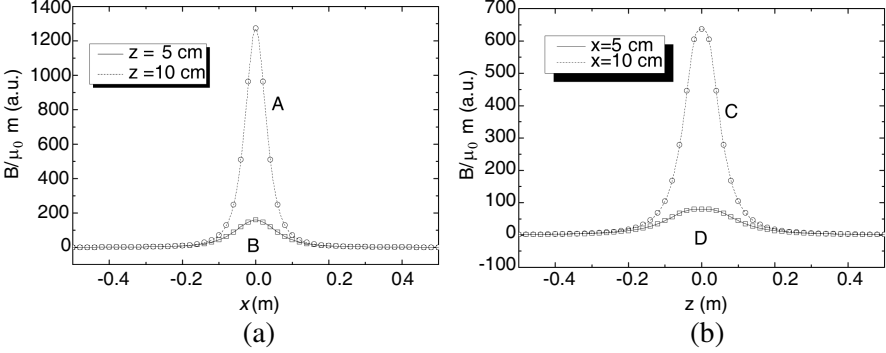


Figure 3. Rescaled magnetic field $\sqrt{B_x^2 + B_z^2}/\mu_0 m$ calculated (symbols) with Eqs. (5) and (6) under dipole approximation $|\vec{R}| \gg r$ versus the rescaled analytical expressions (dashed lines and lines). The rescaled magnetic fields are calculated along the (a) x axis and (b) z axis along two axes separating the centre (5 and 10 cm).

3. LOSS OF THE LINEAR MOMENTUM

Assumptions must be given on the dimensionality of the system. Typical length scales are the size of the emitter and receptor rings, their separating distance, and the typical wavelength corresponding to the working frequency. The standard actuators have typically an emitter-to-receptor distances z around the millimeter, which involves that the electromagnetic wavelength participating in the force is at maximum in the order of millimeter. Longer wavelengths cannot excite electrons on the metal participating in the total force. However, other contribution might come from the dimension of the system d which is typically at maximum in the order of decimetre. The frequency f to treat must be higher than the threshold frequency $f > f_{th} = c/d \approx 3 \text{ GHz}$ in vacuum. This relatively high threshold frequency justifies the use of Jefimenko equations [16]. The Eqs. (4)–(6) take into account the fact that in the transient regime the waves emitted by different parts of the emitter reach different parts of the receptor and these in retarded regime, by integrating all the spatial and temporal effects. However, the calculation of eddy currents is far to be trivial. The skin depth ζ of eddy currents in transient regime is written as $\zeta(t) = \sqrt{4t/\sigma\mu_r\mu_0}$ [17]. σ and μ_r are the electronic conductivity and relative magnetic permeability, respectively. Note in the transient regime, the skin depth ζ does not depend on the frequency, but on the time t . Let's consider thus the interaction between two coaxial rings,

as shown in inset of Fig. 5. The magnetic field B_1 is produced at a time $t = 0$ by means of transient current i_1 . It leaves the emitter ring, covers the ring-to-ring distance z_0 at light speed and starts inducing the current i_2 in the receptor ring at a time $t = z_0/c$. A Laplace force $\vec{F}_{21} = i_2 \oint \vec{dl}_2 \wedge \vec{B}_1$ is created in the receptor ring. The Laplace

force is the particular case of Lorentz force for a current distribution and both are valid in transient regimes. i_2 must be determined from the induced electromotive force $E = L_2 di_2/dt + R_2 i_2 = -\partial\Phi_{B2}/\partial t$ where L_2 , R_2 and Φ_{B2} are respectively the inductance, resistance and magnetic flux of the receptor ring. In the situation of a transient current pulse $z_0/c \ll L_2/R_2$, the inductance term is dominant and the current is simply $i_2 \approx -\Phi_{B2}/L_2$. The field B_2 , produced by i_2 , covers back the ring-to-ring distance and modifies the current inside the emitter ring at a time $t = 2z_0/c + \delta$ (δ is a minor delay due to slowing light speed into the metallic crystal of the receptor ring). Now the emitter ring is subject to the force \vec{F}_{12} starting at $t = 2z_0/c + \delta$, and so on. Note that both \vec{F}_{12} and \vec{F}_{21} are times dependent. If the emitter and receptor rings are jointly attached, the resultant of the system $\vec{R} = \vec{F}_{12} + \vec{F}_{21}$ can be calculated in ranges of times. The normalized instantaneous resultants $R_z^{(n)}$ along z axis are shown below for the first three ranges of times $\Delta t^{(n)}$ where n indexes the wave front travel. The initiating transient current i_1 starts at $t = 0$:

$$\Delta t^{(1)} = [0; z_0/c) \quad R_z^{(1)} = |F_{21}| - |F_{12}| = 0 \quad (7)$$

$$\Delta t^{(2)} = [z_0/c; 2z_0/c + \delta) \quad R_z^{(2)} \approx \left| 2\pi r_2 B_{\rho 1} \int \vec{B}_{z1} d\vec{S}_2 / L_2 \right| - 0 \quad (8)$$

$$\Delta t^{(3)} = [2z_0/c + \delta; 3z_0/c + \delta) \\ R_z^{(3)} \approx \left| 2\pi r_2 B_{\rho 1} \int \vec{B}_{z1} d\vec{S}_2 / L_2 \right| - \left| \left(i_1 - \int \vec{B}_{z2} d\vec{S}_1 / L_1 \right) 2\pi r_1 B_{\rho 2} \right| \quad (9)$$

where $B_{\rho 1}$, B_{z1} , $B_{\rho 2}$ and B_{z2} are calculated using Eqs. (5) and (6). The induced currents i_1 and i_2 decrease versus time and finally will not significantly contribute to the final force \vec{R} . The maximum instantaneous resultant is reached in the first receptor-to-emitter electromagnetic wave travel $\Delta t^{(2)} = [z_0/c; 2z_0/c + \delta)$. After this range of time, switches simultaneously opening the emitter and receptor circuits or an adequate signal would reset to zero the currents. Consequently, they annihilate the Laplace forces F_{12} and F_{21} . When after deriving Eqs. (5) and (6), which account all the dynamics of the electromagnetic field, Eqs. (7)–(9) give the net force versus time and wave front travel which Eqs. (5) and (6) do not give. To circumvent the

space scale issues, a magnetic core will be introduced in the discussion part.

Thus, a current pulse into the emitter ring applied during $2z_0/c + \delta$ and a subsequent opening of emitter and receptor circuits create a maximum net force $R_z^{(2)} = |F_{21}|$. The fast opening of circuits will create an induction that will prolong the waiting time by t_{s-i} before imposing a new pulse into the emitter ring. In short, to continuously get a net force $R_z^{(2)} = |F_{21}|$, a current ramp should be applied during $2z_0/c + \delta$ at a frequency $f = 1/(3z_0/c + \delta + t_{s-i})$. To get a reasonable thrust $R_z^{(2)}$ in vacuum, calculations showed a working distance and frequency at respectively $z_0 = 0.1$ mm and $f = 1$ THz, the latter frequency is out of current possibilities. The resultant is interesting if only it can be used not only on time scales of current pulses (typically ns), but on much longer time scales. The fundamental question is to check the validity of interrupting the current loops to get a zero force without inducing a counter-induction. Before having a second current pulse, a subsequent waiting time must get rid of remaining fields and also of remaining counter-forces. In practice, the ultra fast current switches can be made using field effect transistors (FETs) [18], ultra fast actuators running at most at 1 GHz [19] or even semiconductor junctions [20]. All three should run at very high frequencies.

Clearly, the inertial coil-ring system moves in one direction without applying external forces. The question raised in the introduction is answered: a thrust is created in the coil-ring system using retarded fields. An adapted electronics can force the system to move not only after one current ramp, but also after series of current ramps. A possible explanation of the observed loss of the mechanical linear momentum is the loss of the so-called electromagnetic momentum. The electromagnetic waves exert a pressure, and it is expressed in static regime as follows $P = \varepsilon_0 \varepsilon_r E^2 / 2 + B^2 / 2 \mu_0 \mu_r$ [13]. The total pressure P present in the coil-ring system is not symmetric, i.e., the coil exerts an electromagnetic pressure on the ring placed on only one side of the coil. In the other side of the coil, the pressure exerted in vacuum is lost and is likely responsible for the observed loss of the mechanical linear momentum. An additional explanation of the loss of the momentum is the internal heating. In brief the eddy currents created in the receptor ring by high frequency electromagnetic waves will be themselves source of electromagnetic waves. However, the spectrum covered by these induced waves likely contains infrared light since thermal heating accompanies eddy currents in metals. To avoid parasitic electromagnetic crosstalk, a special care must be done on a proper electrical shielding of current leads.

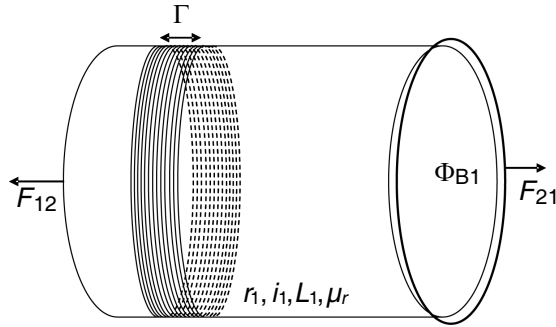


Figure 4. Cylindrical magnetic core placed inside the emitter coil. The receptor ring is placed outside the magnetic core. See text for more info.

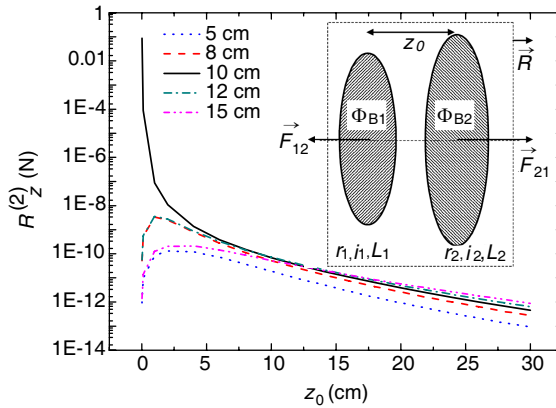


Figure 5. Numerically calculated instantaneous net force $R_z^{(2)}$ (in N) for a system of emitter-receptor vs. their separating distance z_0 and for different receptor radius r_2 . The emitter radius was taken $r_1 = 10$ cm, a receptor ring inductance $L_2 = 10$ mH, a magnetic core with $\mu_r = 10$. The current i_1 was applied with a ramp of 50 mA/ns. The inset shows the interaction of two coaxial emitter (left) and receptor (right) rings. Φ_{B1} , Φ_{B2} are the magnetic fluxes, \vec{F}_{21} , \vec{F}_{12} the Laplace force for the receptor and emitter rings respectively. The outer dashed box represents the system of jointed rings with an instantaneous resultant $\vec{R} = \vec{F}_{12} + \vec{F}_{21}$. The inset does not show the magnetic core for simplicity.

To summarize, the typical working frequencies should not exceed hundreds of GHz due to the mentioned technical limitations of switches. The next section discusses a way to reduce the working frequency by introducing a magnetic core.

4. DISCUSSION ON A REAL THRUSTER

An option to decrease the frequency $f = 1$ THz in order to have a workable frequency without losing the amplitude of thrust $R_z^{(2)}$ is to use a coaxial magnetic guide material with a high magnetic permeability μ_r as shown in Fig. 4. For clarity, the current power supply, the electronics and the support implemented are not represented. In the end, they will affect the total mass, and consequently the effective work and yield. The receptor ring is placed in vacuum, in the end of the core, and therefore its received magnetic field has to be described in vacuum only. The internal field of the magnetic core will create a phase delay δ' , discussed in detail below. At high frequencies the treatment of magnetic field inside a core is simpler using complex permeability equations than using brutal finite element calculations such as the Schwarz-Christoffel mapping [21]. At high frequencies, the magnetic field can be decomposed as $H = H_0 e^{j\omega t}$ in a core and $B = B_0 e^{j(\omega t - \delta')}$ in vacuum. The permeability in transient regime is then deduced

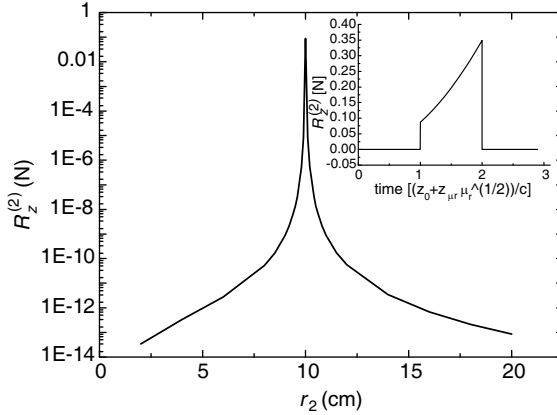


Figure 6. Numerical instantaneous resultant $R_z^{(2)}$ vs. receptors radius r_2 , for an emitter-receptor distance $z_0 = 0.1$ mm and an emitter radius $r_1 = 10$ cm. The inset of Fig. 3 shows a full period of the calculated thrust $R_z^{(2)}$ versus time with $r_1 = r_2 = 10$ cm, $L_2 = 10$ mH, $z_{\mu r} = 10$ cm and $N_s = 140$.

as $\mu \equiv B/H = B_0/H_0 e^{-j\delta'} = \mu' - j\mu''$ where $\mu' = B_0/H_0 \cos \delta'$ and $\mu'' = B_0/H_0 \sin \delta'$ [22]. δ' is an intrinsic value of magnetic materials and is associated with losses (such as hysteresis or eddy currents), e.g., in static regime $\delta' = 0$. An analytical treatment [22] gives the loss factor $\tan \delta' = \omega\tau\xi/(1 + \omega^2\tau^2 + \xi)$ where τ and ξ are respectively the relaxation time of magnetic domains and constant depending on magnetic susceptibility, under transient magnetic field. While ω increases, especially for high frequencies, the loss factor $\tan \delta'$ becomes small and the remaining losses are attributed by eddy currents losses. They can be avoided by reducing the dimension of the core in one dimension (hysteresis losses are also reduced at high frequencies). According to the Fig. 4, the path followed by the magnetic field suggests that the section at the end of cylinder can be attributed to a coil without core where the flux Φ_{B1} remains the same through the cylinder. As discussed above, the losses are tiny $\tan \delta' \approx 0$ within the range of frequencies involved ($f > 3$ GHz) and such magnetic materials firstly decrease the light speed by a factor $\sqrt{\mu_r \epsilon_r}$ and secondly act as a spacer of length $z_{\mu r}$ between the two rings. The total distance separating the two rings is then $z_0 + z_{\mu r}$ where the receptor ring is placed at z_0 from the end of a cylindrical magnetic core. Then, a current ramp should be applied during $2(z_0 + \sqrt{\mu_r z_{\mu r}})/c + \delta$ at frequency $f = 1/(3(z_0 + \sqrt{\mu_r z_{\mu r}})/c + \delta + t_{s-i})$. Moreover, for a number N_s of emitter rings, $R_z^{(2)}$ is proportional to N_s^2 and a time delay Γ/c should be taken into account where Γ is the spatial elongation of N_s wires, see Fig. 4. At $t = (z_0 + \sqrt{\mu_r z_{\mu r}})/c$, $R_z^{(2)}$ were numerically calculated using Eqs. (5), (6) and (8), e.g., for an emitter ring radius $r_1 = 10$ cm, a receptor ring inductance $L_2 = 10$ mH, and $z_{\mu r} = 10$ cm, $\Gamma = 2$ mm, $\mu_r = 20000$ and $N_s = 140$ (Fig. 5). $\Gamma/z_{\mu r} = 2\%$ means that the time delay due to spatial elongation Γ is considered small compared to the delay of coil-to-ring distance. The current i_1 was applied with a ramp of 50 mA/ns. $R_z^{(2)}$ were calculated versus z_0 and for different receptor radius r_2 . A maximum force is shown when the two rings have equal radius. When the receptor ring is near the magnetic core ($z_0 = 0.1$ mm), Fig. 6 shows a maximum of $R_z^{(2)} \approx 0.1$ N for $r_1 = r_2 = 10$ cm. The inset of Fig. 6 shows a full period of the calculated thrust $R_z^{(2)}$ versus time. The maximum attainable force is $R_z^{(2)} \approx 0.35$ N. The abrupt force at $t = (z_0 + \sqrt{\mu_r z_{\mu r}})/c$ is due to $\partial i/\partial t \neq 0$ in Eqs. (5) and (6). The low forces in the present thruster with $N_s = 140$ are competitive with other existing thrusters [1]. For instance, electrostatic propulsion system based on Xenon ions reveals a thrust of 0.2 N. Pulsed plasma using Teflon[®] shows a thrust of 0.1 N. The main advantage of the present thruster is the direct conversion of electricity to kinetic

energy without using propellant. There is an way to increase the thrust by increasing N_s . For higher N_s , the delay due to the spatial elongation Γ cannot be ignored any more. The force of 130000 N was reached [2] using much higher turns N_s and running a longer time of current ramp, obtaining then higher magnetic fields. Typically, the current reached was about 1800 A, the number of turns per length unit 1358 turns/m and the ramp time was about hundreds of μs . Moreover, the possibility to play with dimensions, transient currents and magnetic cores help the experimental feasibility.

5. CONCLUSION

In conclusion, the generalized equations of Jefimenko for the single ring with a transient current show good agreement with the Biot-Savart expression in static regime. A second validation is the good agreement between analytical and numerical calculations in the dipole moment approximations. Due to dimensionality, the frequencies f involved in the resultant force are higher than the threshold frequency $f > f_{th} \approx 3 \text{ GHz}$ in vacuum. This relatively high threshold frequency justifies the use of Jefimenko equations. To circumvent space and time scale issues, a magnetic core is introduced. The introduction of a magnetic core creates a phase delay δ' that is shown to be small. The simulations of instantaneous forces between emitter and receptor rings show the existence of a net thrust in one direction for a small time slot. A direct consequence is a possible loss of the linear momentum. The thermal heating and more likely the asymmetrical electromagnetic pressure exerted in the coil-ring system are responsible for the loss. To benefit of a maximum net electromagnetic thrust $\vec{R} = \vec{F}_{21}$, the emitter circuit should be opened before receiving the magnetic response of the receptor ring. This latter might be opened at the same time to avoid counter-induction effects. The experimental requirements are high frequency signals switches into the emitter and receptor circuits. A thrust of $R_z^{(2)} \approx 0.35 \text{ N}$ was obtained for $N_s = 140$.

REFERENCES

1. Tajmar, M., *Advanced Space Propulsion Systems*, Springer-Verlag, Wien, New York, 2002.
2. Zieve, P. B., J. L. Hartmann, and J. K. Ng, "High force density eddy-current driven actuator," *IEEE Transactions on Magnetics*, Vol. 24, 3144–3146, 1988.

3. Jefimenko, O. D., *Causality, Electromagnetic Induction and Gravitation*, Electret-Scientific-Company, West Virginia, 2000.
4. Jefimenko, O. D., *Electricity and Magnetism*, Appleton-Century Crofts, New York, 1966.
5. Monaghan, J. J., "Heaviside-Feynman expression for fields of an accelerated dipole," *J. Phys. A*, Vol. 1, 112, 1968.
6. Mayes, C. and G. Hoffstaetter, "Exact 1D model for coherent synchrotron radiation with shielding and bunch compression," *Phys. Rev. ST Accel. Beams*, Vol. 12, 024401, 2009.
7. Barut, A. O., "Electrodynamics in terms of retarded fields," *Phys. Rev. D*, Vol. 10, 3335–3336, 1974.
8. Teitelboim, C., D. Villarroel, and C. G. van Weert, "Classical electrodynamics of retarded fields and point particles," *Rivista Del Nuovo Cimento*, Vol. 3, 1–64, 1980.
9. Villarroel, D., "Preacceleration in classical electrodynamics," *Phys. Rev. E*, Vol. 66, 046624, 2002.
10. Heras, J. A., "Radiation-fields of a dipole in arbitrary motion," *Am. J. Phys.*, Vol. 62, 1109–1115, 1994.
11. Heras, J. A., "Explicit expressions for the electric and magnetic fields of a moving magnetic dipole," *Phys. Rev. E*, Vol. 58, 5047–5056, 1998.
12. Jiménez, J. L., I. Campos, and N. Aquino, "Exact electromagnetic fields produced by a finite wire with constant current," *Eur. J. Phys.*, Vol. 29, 163–175, 2008.
13. Jackson, J. D., *Classical Electrodynamics*, John Wiley & Sons, New York, 1999.
14. Griffiths, D. J. and M. A. Heald, "Time-dependent generalizations of the Biot-Savart and Coulomb laws," *Am. J. Phys.*, Vol. 59, 111–117, 1991.
15. Purcell, E. M., *Electricity and Magnetism Berkeley Physics Course*, Vol. 2, McGraw-Hill, New York, 1985.
16. The coil-ring system can be seen as an antenna and the total momentum deduced from the specific spectral band. However, the spectral band calculated from a transient profile of $i(t)$ in retarded coordinates was out of computational limits.
17. Krawczyk, A. and J. A. Tegopoulos, *Numerical Modelling of Eddy Currents*, Oxford University Press, New York, 1993.
18. Weinzierl, S. R. and J. P. Krusius, "Heterojunction vertical FETs revisited — Potential for 225-GHz large-current operation," *IEEE Trans. Electron Devices*, Vol. 39, 1050–1055, 1992.
19. Ekinici, K. L. and M. L. Roukes, "Nanoelectromechanical

- systems,” *Rev. Sci. Instrum.*, Vol. 76, 061101, 2005.
20. Lyubutin, S. K., S. N. Rukin, B. G. Slovikovsky, and S. N. Tsyranov, “Ultrafast current switching using the tunneling-assisted impact ionization front in a silicon semiconductor closing switch,” *Tech. Phys. Lett.*, Vol. 31, 196–199, 2005.
 21. Markovic, M., M. Jufer, and Y. Perriard, “Analytical force determination in an electromagnetic actuator,” *IEEE Transactions on Magnetics*, Vol. 44, 2181–2185, 2008.
 22. Getzlaff, M., *Fundamentals of Magnetism*, Springer-Verlag, Berlin and Heidelberg, 2008.